Ceramics International **24** (1998) 497–506

PII: S0272-8842(97)00048-5
0272-8842/98 $19.00 + .00

Tough and Strong Ce-TZP/Alumina Nanocomposites Doped with Titania

Masahiro Nawa,[a]* Syoichi Nakamoto,[a] Tohru Sekino[b] & Koichi Niihara[b]

[a]Central Research Laboratory, Matsushita Electric Works, Ltd, 1048, Kadoma, Osaka 571, Japan
[b]The Institute of Scientific and Industrial Research, Osaka University, 8-1, Mihogaoka, Ibaraki, Osaka 567, Japan

(Received 13 May 1997; accepted 17 June 1997)

Abstract: To develop a new attractive Ce-TZP ceramic, which possesses a high strength while still preserving significant high toughness, we investigated an intragranular type of nanocomposite in lower CeO_2 content for 0–1 mol% TiO_2 doped Ce-TZP/Al_2O_3 system. These composites partly possessed an intragranular microstructure, in which several of 10–100 nm sized Al_2O_3 particles were trapped within the ZrO_2 grains. Furthermore, elongated Al_2O_3-like phases were produced at the ZrO_2 grain boundaries, which were in-situ precipitated during the sintering process. TiO_2 was confirmed to dissolve into the tetragonal ZrO_2 lattice, which was determined to be effective for strengthening with a slight addition due to its grain growth enhancing ability on ZrO_2. For an optimum component with 0.05 mol% TiO_2 doped 10Ce-TZP/30 vol% Al_2O_3 composite, both high strength (950 MPa) and high toughness (18.3 MPa.$m^{1/2}$ for the IF method, 9.8 MPa.$m^{1/2}$ for the SEVNB method) were achieved thus breaking through the strength–toughness tradeoff relation in transformation toughened ZrO_2 and its composite materials. ©1998 Elsevier Science Limited and Techna S.r.l.

1 INTRODUCTION

CeO_2 stabilized tetragonal zirconia polycrystals (Ce-TZP) show a very high toughness[1] and a complete resistance to low temperature aging degradation[2] in comparison to those of Y_2O_3 stabilized tetragonal zirconia polycrystals (Y-TZP). However, the attractive properties are accompanied by a modest strength and a modest hardness. For example, Ce-TZP containing 8–12 mol% CeO_2[3] exhibits an extremely high toughness of 10–20 MPa $m^{1/2}$, but show a modest hardness of 8 GPa and a low strength of 600–800 MPa even for an optimum component of 12 mol% CeO_2 content. Consequently, if Ce-TZP successfully achieved both high strength and high hardness, they would be expected to be the candidate for a new attractive TZP ceramic, which overcomes an essential fault of Y-TZP suffering from low temperature aging degradation.

To compensate the disadvantages of lower strength and lower hardness in Ce-TZP, recent investigations have been focused on 12 mol% Ce-TZP/Al_2O_3 composites. In the 12Ce-TZP/30–50 vol% Al_2O_3 composites, strength has improved up to 900 MPa. However, toughness decreased remarkably from 20 to 5.5 MPa $m^{1/2}$ with increasing Al_2O_3 content.[4] Thus, it was proved that further addition of the second phase resulted in the inevitable decrease of the toughness due mainly to the restraint of the tetragonal-to-monoclinic transformation. To restrain the toughness degradation of the composite caused by the addition of the second phase, the form controls of Al_2O_3 particles have been investigated. It was shown that the toughness can be improved by incorporation of the elongated and/or plate-like Al_2O_3 phases which were produced in situ sintering by the addition of a small amount of metal oxides[5,6] or dispersing

*To whom correspondence should be addressed at: Central Research Laboratory, Matsushita Electric Works, Ltd. 1048, Kadoma, Osaka 571, Japan. Fax: +81-6-904-7104; e-mail: nawa@crl.mew.co.jp

lanthanum-β-aluminate crystals.[7] However, the formations of micrometer sized elongated and/or plate-like phases were not always effective to improve the strength due to the enlargement of a flaw size in the composites. On the contrary, using Ce-TZP of less than 12 mol% CeO_2 as a ceramic matrix would be effective for the restraint of the toughness degradation of the composites. Because they show a significant higher toughness value than that of 12Ce-TZP,[1] although they still have an essential fault of lower strength. Therefore, it is a serious point of contention whether or not a significant strengthening can be achieved in lower CeO_2 content of Ce-TZP/Al_2O_3 composite.

In recent years, nanocomposites, in which nanometer sized second-phase particles are dispersed within the ceramic matrix grains and/or at the grain boundaries, have been investigated.[8,9] They have shown significant improvement in strength due to a decrease in flaw size associated with the intragranular nano-dispersion. In the previous work, for further strengthening of Ce-TZP, we have applied a general idea of the nanocomposite to 12Ce-TZP/Al_2O_3 composite system.[10] A novel interpenetrated intragranular type of nanocomposite has been successfully fabricated and achieved a significant improvement in strength of 1012 MPa, which restrained the toughness degradation in the minimum level through tailoring the sintering condition.

The purpose of this investigation is to extend the result of 12Ce-TZP/Al_2O_3 nanocomposite to lower CeO_2 content of Ce-TZP/Al_2O_3 composite system, and to develop a new attractive Ce-TZP ceramic, which possesses a high strength while still preserving significant high toughness. Furthermore, the effect of TiO_2 addition on strengthening was also investigated. In the zirconia-rich end of the titania phase equilibrium diagram,[11] TiO_2 is known to dissolve into tetragonal ZrO_2 up to 18 mol% at high temperatures and act as a stabilizing agent in a similar manner to Y_2O_3 and CeO_2. Moreover, there was a report that TiO_2 had an ability to promote a grain growth of ZrO_2. That is, 10 mol% TiO_2 doped 8Y-TZP ceramic had shown the transparent property due to a homogeneous and large grain growth by the action of TiO_2 addition.[12] Therefore, it is expected that TiO_2 addition to the Ce-TZP/Al_2O_3 system would be effective for strengthening from the point of the phase stability of the tetragonal phase and the promotion of intragranular nano-dispersion due to its ability to promote grain growth. The relationship between microstructure and mechanical properties will be discussed.

2 EXPERIMENTAL PROCEDURE

2.1 Fabrication

Ce-TZP powder containing 10–12 mol% CeO_2 (grade OZC-10-12CE, Sumitomo-Osaka Cement Co., Japan) with a specific surface area of $15\,m^2\,g^{-1}$ and TiO_2 powder (grade SP-01, Osaka Titanium Co., Japan) with a specific surface area of $25\,m^2\,g^{-1}$ were used as a starting material for the matrix. In the raw starting Ce-TZP powder, it was apparent that Mg had already been intentionally added (about 0.05 wt%) by the chemical analysis. α-Al_2O_3 powder (grade TM-DAR, Taimei Chemical Co., Japan) with an average grain size of 0.22 μm was used as the secondary dispersions. For binary system, Ce-TZP powder stabilized with either 10,11, or 12 mol% CeO_2 containing 30 vol% Al_2O_3 was ball milled using zirconia media in ethanol for 24 h. The slurries were dried in air and passed through a 250 μm screen. For the series with TiO_2 additions, 10Ce-TZP powder containing either 0, 0.05, 0.2, 0.5 or 1 mol% TiO_2 was ball milled with 30 vol% Al_2O_3 powder. Then the mixtures were dried and calcined at 1000°C for 1 h to dissolve TiO_2 into ZrO_2. Calcined powders were further milled in ethanol for 24 h and dried. For all powder mixtures, green compacts were prepared by uniaxial die pressing at 10 MPa and then isostatic pressing at 150 MPa. The sintering conditions were 1400–1550°C for 2 h.

2.2 Characterization

The densities of the specimens were obtained by the Archimedes method using a toluene medium. Crystalline phases of the composites on the polished surfaces of the specimens were determined by X-ray diffraction analysis (XRD) with CuKα radiation. The tetragonal, monoclinic and cubic phases were evaluated using the analysis of Garvie and Nicholson.[13] Lattice constants of the tetragonal ZrO_2 phase were determined by XRD with CrKα radiation based on the outer standard method using Si powder. The grain size of the composite was estimated by the line intercept method on the thermally etched surfaces. The microstructure of the composites was observed by scanning electron microscopy (SEM) and transmission electron microscopy (TEM).

2.3 Mechanical properties

The sintered specimens were cut by a diamond blade saw, and ground with a 600-grit diamond wheel. The specimens, having dimensions of

3×4×40 mm, were subjected to the elastic modulus measurement and mechanical property tests. The elastic modulus was determined by the resonance vibration method. The fracture strength was measured by a 3-point bending test at room temperature. The span length and cross-head speed were 30 mm and 0.5 mm min^{-1}, respectively. The tensile surfaces of the specimens were polished with a diamond liquid suspension. The fracture toughness was estimated by the indentation-fracture (IF) method using the following equation of Niihara *et al.*[14]

$$K_{IC} = 0.018 Hv a^{1/2} (l/a)^{1/2} (Hv/E)^{-2/5}$$

where Hv is the Vickers hardness and E is the elastic modulus. Here *l* equals to c−a, wherein a and c is the half length of the Vickers impression and the palmqvist crack, respectively. The polished surfaces were used for the Vickers indentation with a load of 490 N and a loading duration of 15 s. Separately, the toughness was also estimated by the single edge V notched beam (SEVNB) method. The V notch was machined using a special diamond slicing wheel, which was developed by Awaji *et al.*[15] The required toughness can be accurately obtained by forming a sharper V-shaped notch with very small root curvature. In this study, the specimens, having a V notch root radius around 10 to 15 μm, were used. The V notched specimens, having dimensions of 3×4×20 mm, were subjected to a 3-point bending test with a span length of 16 mm and a cross-head speed of 0.5 mm min^{-1}. The value of toughness was calculated by using the Srawley's shape coefficient.[16]

3 RESULTS AND DISCUSSION

3.1 Microstructure

Sintered at various temperatures 10–12Ce-TZP/30 vol% Al_2O_3 components primarily consisted of the tetragonal phase and a small amount (less than 3 vol%) of the monoclinic phase. There were no traces of the cubic phase. In the system of 0–1 mol% TiO_2 doped 10Ce-TZP/30 vol% Al_2O_3 composites, the identical crystalline phases were detected.

The representative TEM image of the 10Ce-TZP/30 vol% Al_2O_3 composite sintered at 1500°C is shown in Fig. 1. It was confirmed that an intragranular type of microstructure was developed in the Ce-TZP/Al_2O_3 composite system, in which several of 10–100 nm sized Al_2O_3 particles were

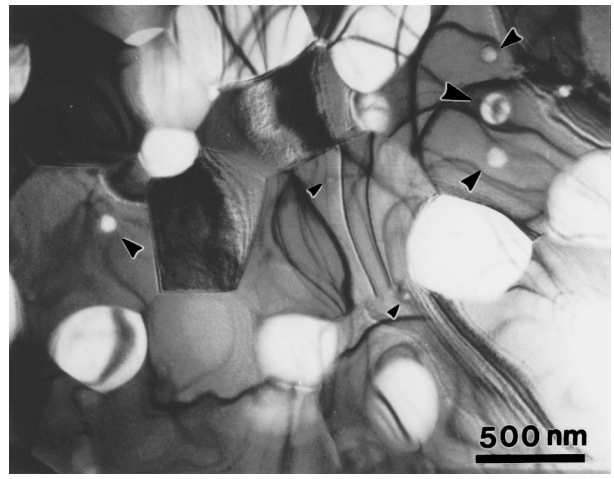

Fig. 1. TEM image of the microstructure for the 10Ce-TZP/30 vol% Al_2O_3 composite sintered at 1500°C.

trapped within the ZrO_2 grains. Furthermore, two kinds of intragranular Al_2O_3 dispersions are shown in Fig. 2. One is a typical nano-dispersion. That is, several 10 nm sized Al_2O_3 particle were located within the ZrO_2 grain, which is considered to be trapped during the initial sintering stage as reported before.[8,9] On the other side, relatively larger Al_2O_3 particle of about 300 nm were located at triple junctions, which is supposed to be trapped into the ZrO_2 grains due to the grain boundary disappearance during the intermediate sintering stage.

As another aspect of the microstructure, SEM photographs of thermal-etched surfaces of the 10Ce-TZP/30 vol% Al_2O_3 composite sintered at 1500°C are shown in Fig. 3. It was recognised that an unexpected elongated Al_2O_3-like phase was presented at the ZrO_2 grain boundaries. Identical copies of the elongated Al_2O_3-like phases were also observed for every 0.05, 0.2, 0.5 or 1 mol% TiO_2 doped 10Ce-TZP/30 vol% Al_2O_3 composites in the similar distribution ratio. The results of the energy dispersive X-ray analysis (EDAX) along with TEM image corresponding to the point of the analysis is shown in Fig. 4. For the elongated Al_2O_3-like phase, Ce and Mg (included in the starting Ce-TZP powder) as well as Al were detected, whereas Mg was not found at all within both Al_2O_3 and ZrO_2 grains. In the system of using Ce-TZP powder without MgO, such an elongated phase was not presented. Judging from these results, it was suggested that this elongated phase might be a complex oxide resulting from a reaction between Al_2O_3, CeO_2 and MgO, although such a bi-product was not detected by the XRD analysis. The composition of this elongated phase was not clear, but was assumed to be magnetoplumbite type ($Ce^{3+}Mg^{2+}Al_{11}O_{19}$) of crystal.[5]

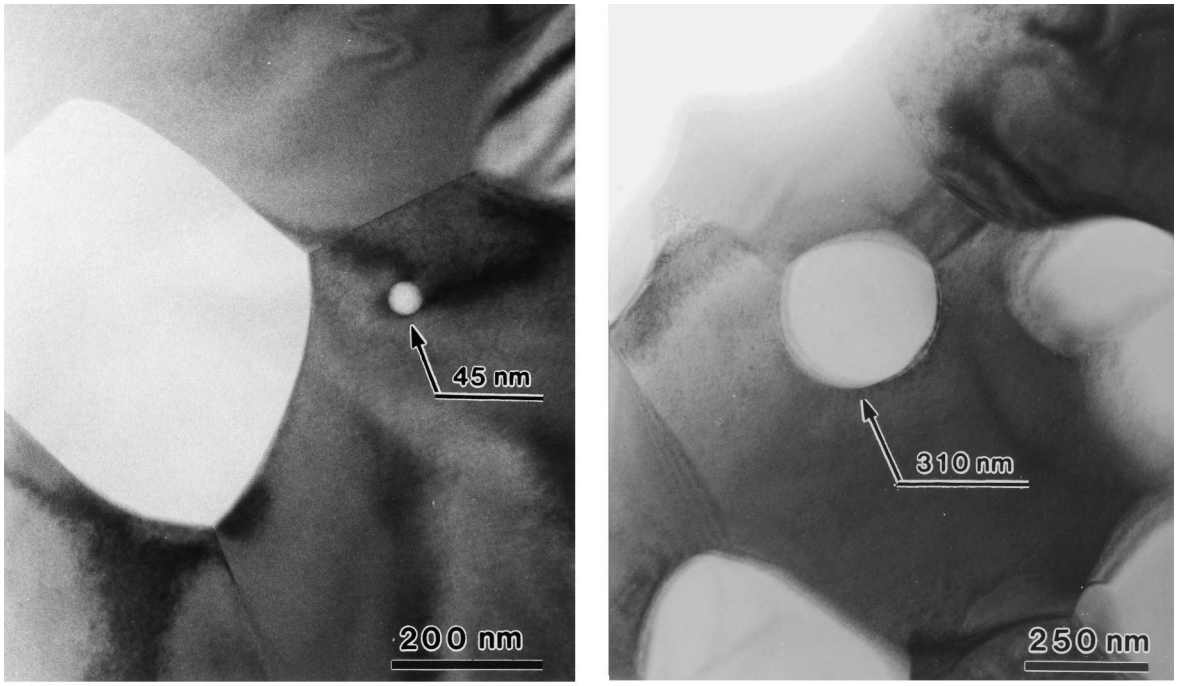

Fig. 2. TEM images of the different sized Al_2O_3 particles trapped within the zirconia grains for the 10Ce-TZP/30 vol% Al_2O_3 composite sintered at 1500°C: (a) several 10 nm sized Al_2O_3 particles, (b) larger Al_2O_3 particle of about 300 nm.

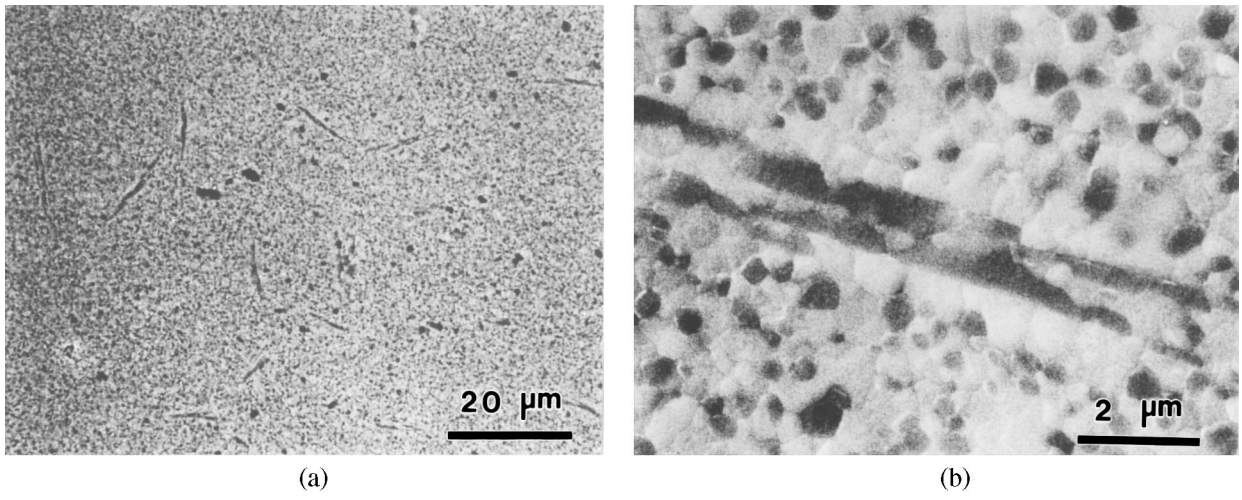

Fig. 3. SEM photographs of thermal-etched surfaces for the 10Ce-TZP/30 vol% Al_2O_3 composite sintered at 1500°C: (a) microstructure including elongated Al_2O_3-like phases, (b) at higher magnification.

3.2 Mechanical properties

3.2.1 The effect of CeO_2 content

The fracture strength as a function of CeO_2 content for both monolithic 10–12 mol% Ce-TZP and its based Ce-TZP/30 vol% Al_2O_3 composites is shown in Fig. 5. The existence of a positive relation between CeO_2 content and strength was ascertained for both monolithic Ce-TZP and its based composites. Furthermore, the substantial improvement in strength was presented for the 10–12 mol% Ce-TZP/30 vol% Al_2O_3 composites. They exhibited 1.5 times higher strength than those of each monolithic Ce-TZP. The average grain size of the composite was reduced below 0.7 μm, in contrast with that of the monolithic Ce-TZP of about 1.0–1.3 μm. This strengthening was determined to be the result of two relating factors. The first concerns a decrease in a flaw size accompanying the intragranular microstructure. That is, several 10–100 nanometer sized Al_2O_3 particles, which are trapped within the ZrO_2 grain, are believed to have a role in dividing a grain size into more finer sized particles. The second factor concerns the stress induced

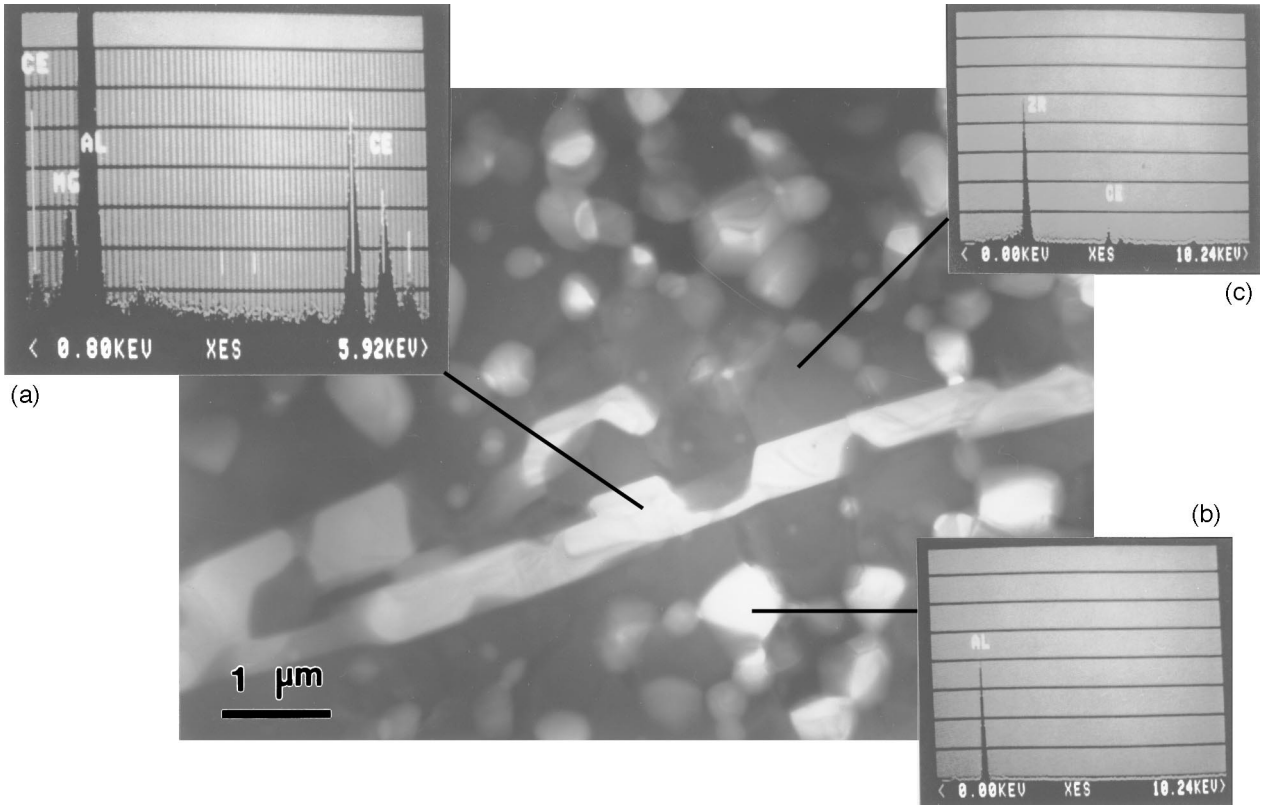

Fig. 4. The results of the EDAX analysis along with TEM image corresponding to the point of the analysis for the 1 mol% TiO_2 doped 10Ce-TZP/30 vol% Al_2O_3 composite sintered at 1500°C: (a) elongated Al_2O_3-like phase, (b) Al_2O_3 grain, (c) ZrO_2 grain.

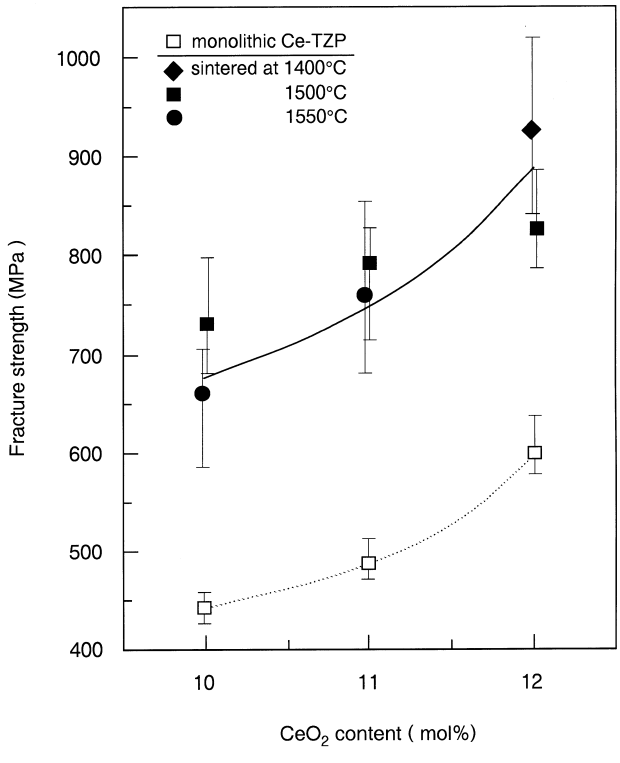

Fig. 5. The fracture strength as a function of CeO_2 content for both monolithic 10–12 mol% Ce-TZP and its based Ce-TZP/30 vol% Al_2O_3 composites sintered at various temperatures.

phase transformation on strengthening for TZP ceramics. It has been apparent that the retention of the tetragonal phase is critically governed by the grain size.[17] Hence, reduction of the grain size is predicted to increase the critical stress that induces the tetragonal-to-monoclinic transformation, which leads to augmentation of the strength of TZP ceramics.[18]

The fracture toughness as a function of CeO_2 content for both monolithic 10–12 mol% Ce-TZP and its based Ce-TZP/30 vol% Al_2O_3 composite, which was evaluated by the IF method and the SEVNB method, is shown in Fig. 6. For the Ce-TZP ceramics, the values of the toughness estimated by the IF method may be disposed to overestimate due to the large transformed zone about the Vickers indentation[19] and the elongated transformed zone forming ahead of the crack tip.[20,21] Recently, we have reported a large difference in the toughness value measured by the IF and SEVNB method for the 12Ce-TZP/Al_2O_3 composites.[10] The toughness value measured by the IF method has been inclined to increase with an applied load (from 98 N to 490 N) of Vickers indent, which might be due to the rising R-curve behaviour.[22] Furthermore, the large transformation

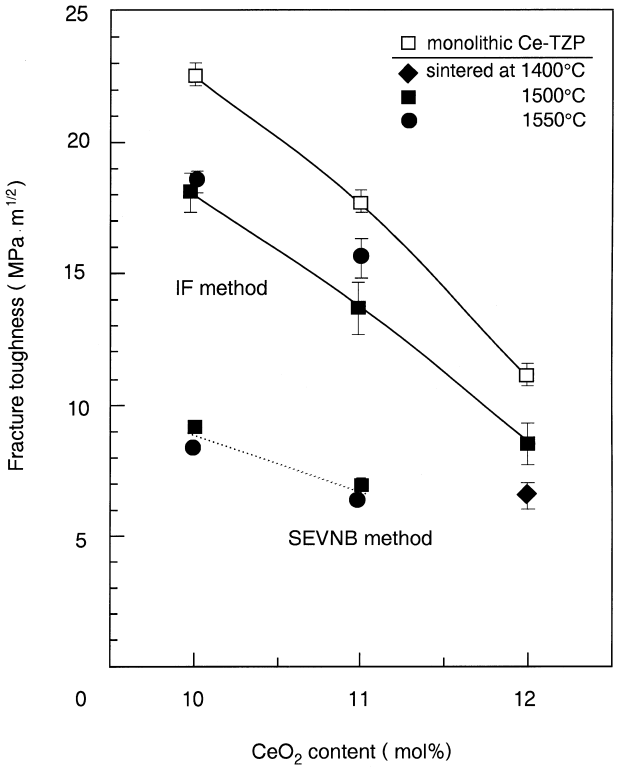

Fig. 6. The fracture toughness as a function of CeO_2 content, which was evaluated by the IF and the SEVNB method, for both monolithic 10–12 mol% Ce-TZP and its based Ce-TZP/30 vol% Al_2O_3 composites sintered at various temperatures.

zone developed about a 490 N Vickers indent has been recognised by the observation of Nomarski interference image. Therefore, the toughness value of the IF method with a load of 490 N has been determined to correspond to the increased stage of toughness in its strong rising R-curve, which was governed by the well developed process zone. On the contrary, the toughness estimated by the SEVNB method has been verified to evaluate a crack initiation behaviour by eliminating rising R-curve.[15] Consequently, it can be concluded that the factors mentioned above play an important role in causing the large difference in the measured toughness between the IF and SEVNB method. As for the dependence of CeO_2 content on the toughness, it was ascertained that the much higher toughness value was obtained with decreasing CeO_2 content of 10 mol%; while the toughness was decreased by the addition of 30 vol% Al_2O_3 for each CeO_2 content, and showed a reduction of about 20% (for the IF method) as compared to that of monolithic Ce-TZP. Whereas, Ce-TZP/30 vol% Al_2O_3 composites containing 10 mol% CeO_2 still preserved higher toughness values of 18.8 MPa $m^{1/2}$ for the IF method, and 9.2 MPa $m^{1/2}$ for the SEVNB method, respectively.

The elastic modulus and the Vickers hardness as a function of CeO_2 content for both monolithic 10–12 mol% Ce-TZP and its based composites are shown in Figs 7 and 8, respectively. Both coefficients substantially improved by the addition of 30 vol% Al_2O_3 in accordance with the linear rule of mixtures, whereas the influence on CeO_2 content was not apparently recognised. The improved hardness value of 11–12 GPa was equivalent to that of Y-TZP.

3.2.2 The effect of TiO_2 doping

The effect of TiO_2 addition (0, 0.05, 0.2, 0.5 or 1 mol%) on further strengthening was examined for the 10Ce-TZP/30 vol% Al_2O_3 composite, which showed a fairly high toughness of 9.2 MPa $m^{1/2}$ (SEVNB), but lower strength of 730 MPa.

The variation of lattice constant and lattice volume of the tetragonal ZrO_2 with TiO_2 content is shown in Fig. 9. It was recognised that both lattice constant and lattice volume decreased with increasing TiO_2 content, except for the 0.05 mol% TiO_2 addition. These results reveal that a titania ion, having a smaller ionic radius than those of Zr^{4+} and/or Ce^{4+}, dissolved into the tetragonal ZrO_2 lattice along with CeO_2, although the exact configuration of the solid solution is not clear. According to the above analysis, it seems reasonable to conclude that TiO_2 addition to the 10Ce-TZP/Al_2O_3 composite would be effective for strengthening from the phase stability of the tetragonal phase due to its ability to act as a stabilizing agent.

The variation of fracture strength with TiO_2 content for the 10Ce-TZP/30 vol% Al_2O_3 composites is shown in Fig. 10. The strength showed a significant increase with a small amount of TiO_2 addition. A maximum strength of 950 MPa was achieved at 0.05 mol% TiO_2 content. The effect of average grain size of ZrO_2 matrix on TiO_2 content for the 0–1 mol% TiO_2 doped 10Ce-TZP/30 vol% Al_2O_3 composites is shown in Fig. 11. The slight grain growth of ZrO_2 matrix from about 0.6 to 0.9 μm was presented with increasing TiO_2 content up to 1 mol%. While a number of finer Al_2O_3 particles within the ZrO_2 grains were frequently observed for the TiO_2 doped 1OCe-TZP/Al_2O_3 composites compared to those of without TiO_2 doping. Consequently, this strengthening at a small range of TiO_2 content was supposed to be caused by TiO_2 acting as a sintering aid and contributing to the promotion of the intragranular nano-dispersion because of its grain growth enhancing ability on ZrO_2.

The variation of fracture toughness with TiO_2 content, which was both evaluated by the IF and

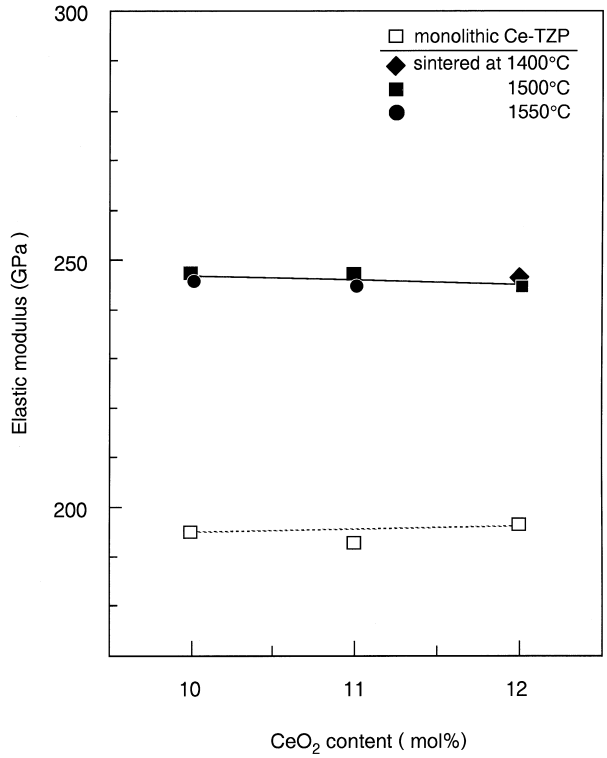

Fig. 7. The elastic modulus as a function of CeO_2 content for both monolithic 10–12 mol% Ce-TZP and its based Ce-TZP/30 vol% Al_2O_3 composites sintered at various temperatures.

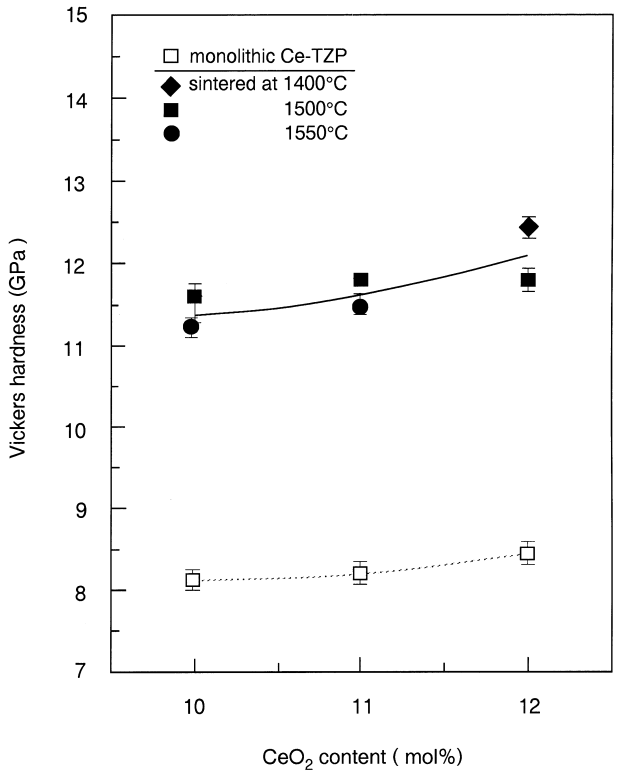

Fig. 8. The Vickers hardness as a function of CeO_2 content for both monolithic 10–12 mol% Ce-TZP and its based Ce-TZP/30 vol% Al_2O_3 composites sintered at various temperatures.

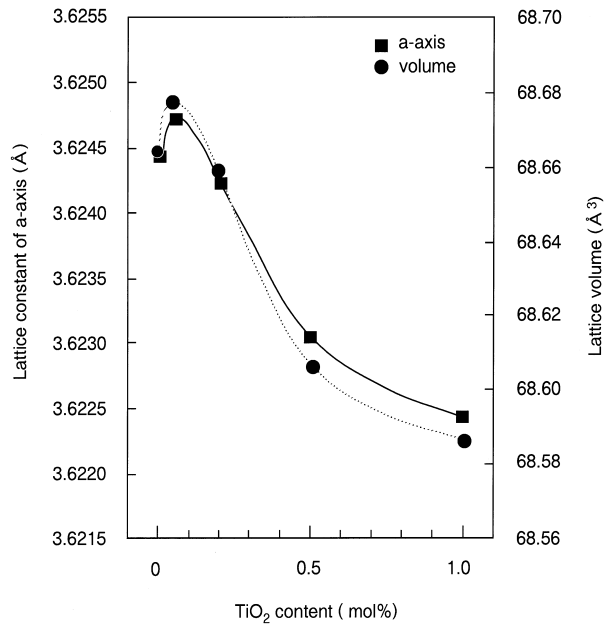

Fig. 9. The variation of lattice constant and lattice volume with TiO_2 content for the 0–1 mol% TiO_2 doped 10Ce-TZP/30 vol% Al_2O_3 composite sintered at 1500°C.

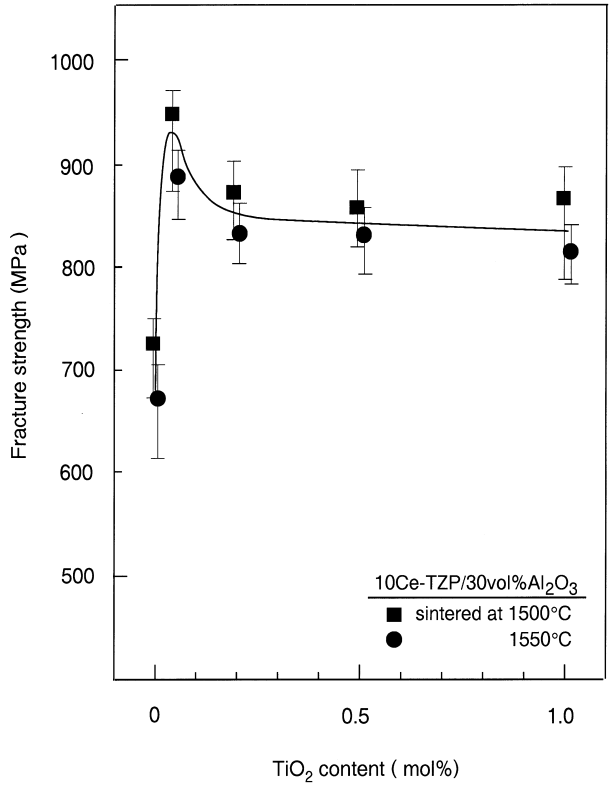

Fig. 10. The variation of the fracture strength with TiO_2 content for the 0–1 mol% TiO_2 doped 10Ce-TZP/30 vol% Al_2O_3 composites.

the SEVNB method, is shown in Fig. 12. The decrease of the toughness is generally predicted when TiO_2 dissolved into tetragonal ZrO_2 as a stabilizing agent due to the restraint of the tetragonal-to-monoclinic transformation. In our recent

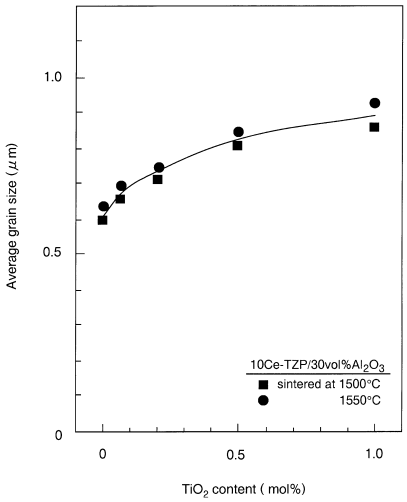

Fig. 11. The effect of average grain size of ZrO_2 matrix on TiO_2 content for the 0–1 mol% TiO_2 doped 10Ce-TZP/30 vol% Al_2O_3 composites.

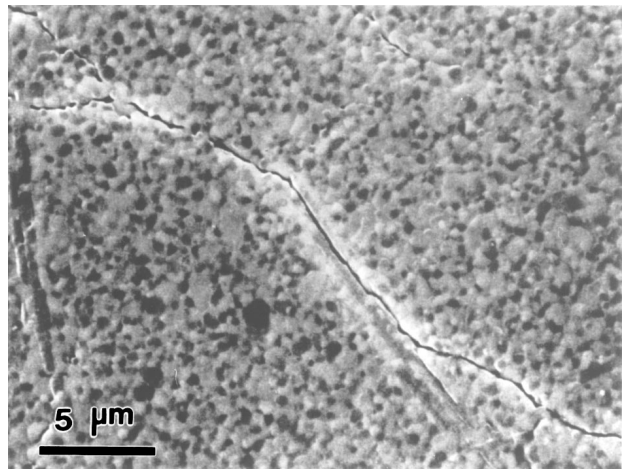

Fig. 13. The crack propagation behaviour around the Vickers indentation for the 0.05 mol% TiO_2 doped 10Ce-TZP/30 vol% Al_2O_3 composite.

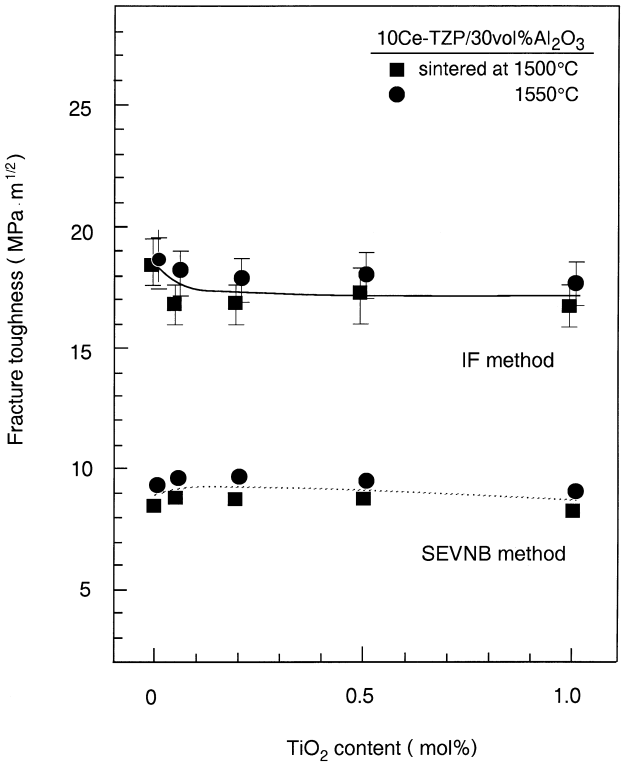

Fig. 12. The variation of the fracture toughness with TiO_2 content, which was evaluated by the IF and the SEVNB method, for the 0–1 mol% TiO_2 doped 10Ce-TZP/30 vol% Al_2O_3 composites.

work on the 0 to 3 mol% TiO_2 doped 12Ce-TZP/30 vol% Al_2O_3 composites,[10] the remarkable decrease of the toughness (9.5 to 6.5 MPa $m^{1/2}$ for the IF method, and 5.4 to 4.8 MPa $m^{1/2}$ for the SEVNB method) has been observed, which corresponded to a decrease of the transformed monoclinic phase. On the contrary, notable decrease of the toughness was not observed in this system up to 1 mol% TiO_2 content. The fracture toughness for the optimum component of the 0.05 mol% TiO_2 doped 10Ce-TZP/30 vol% Al_2O_3 composite maintained almost the same value (18.8 to 18.3 MPa $m^{1/2}$ for the IF method, and 9.2 to 9.8 MPa $m^{1/2}$ for the SEVNB method) as compared to those of the composites without TiO_2 doping. The crack propagation behaviour around the Vickers indentation for the 0.05 mol% TiO_2 doped 10Ce-TZP/30 vol% Al_2O_3 composite is shown in Fig. 13. As seen from this figure, there was definite evidence that a crack propagated round through the in-situ precipitated elongated Al_2O_3-like particle. Consequently, the restraint of the toughness degradation was attributed to the contribution of the crack deflection by the elongated Al_2O_3-like particles.

The variations of the elastic modulus and the Vickers hardness with TiO_2 content for the 10Ce-TZP/30 vol% Al_2O_3 composites are shown in Figs 14 and 15, respectively. The elastic modulus showed a decrease inclination with increasing TiO_2 content and with rising sintering temperature, except for the 0.05 mol% TiO_2 addition. This degradation may be attributed to the solid solution of TiO_2 ion into the tetragonal ZrO_2 lattice, which is the equivalent manner recognising the deterioration in the density. In the case of the Vickers hardness, however, a large degradation was not observed. Both coefficients showed a small increase at a 0.05 mol% TiO_2 content, which corresponded to the component exhibiting a maximum strength. This accordance was believed to be associated with a promotion of the intragranular nano-dispersion, which was derived from a small amount of TiO_2 addition.

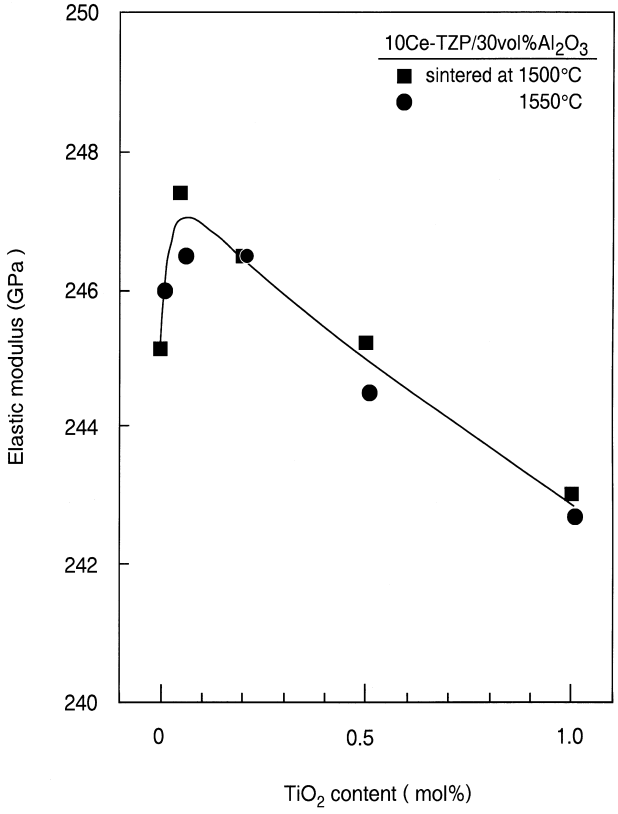

Fig. 14. The variation of the elastic modulus with TiO_2 content for the 0–1 mol% TiO_2 doped 10Ce-TZP/30 vol% Al_2O_3 composite.

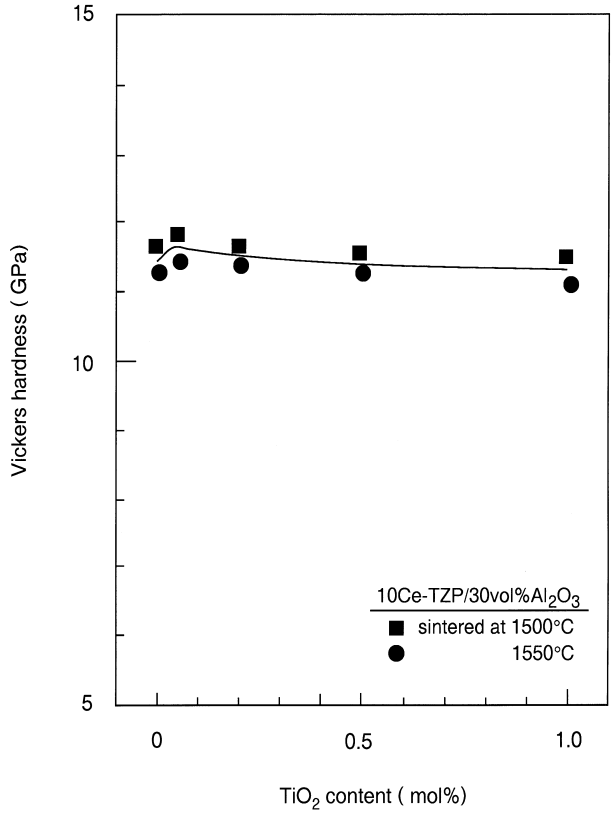

Fig. 15. The variation of the Vickers hardness with TiO_2 content for the 0–1 mol% TiO_2 doped 10Ce-TZP/30 vol% Al_2O_3 composite.

4 CONCLUSIONS

To develop a new attractive Ce-TZP ceramic, which possesses a high strength while still preserving significant high toughness, we investigated an intragranular type of nanocomposite in lower CeO_2 content of Ce-TZP/Al_2O_3 system. In addition, for further strengthening the effect of TiO_2 doping was also examined. The microstructures and their mechanical properties were studied. The results are summarised as follows.

1. 10–12 mol% Ce-TZP/30 vol% Al_2O_3 composites sintered at various temperatures were composed of only ZrO_2 and Al_2O_3 by XRD analysis. Whereas, an elongated Al_2O_3-like phase was presented, which composed of a complex oxide resulting from a reaction between Al_2O_3, CeO_2 and MgO that contained in the starting Ce-TZP powder. In the TiO_2 doped Ce-TZP/Al_2O_3 composite system, the identical crystalline phases were detected. TiO_2 was confirmed to dissolve into the tetragonal ZrO_2 lattice, which was determined to be effective for strengthening with a slight addition due to its grain growth enhancing ability on ZrO_2
2. For the Ce-TZP/30 vol% Al_2O_3 composites with and without TiO_2 doping, the intragranular type of microstructure was developed, in which several of 10–100 nm sized Al_2O_3 particles were trapped within the ZrO_2 grains. Furthermore, an elongated Al_2O_3-like phases were produced at the ZrO_2 grain boundaries, which were in-situ precipitated during the sintering process.
3. For an optimum component with 0.05 mol% TiO_2 doped 10Ce-TZP/30 vol% Al_2O_3 composite, both high strength (950 MPa) and high toughness (18.3 MPa $m^{1/2}$ for the IF method, 9.8 MPa $m^{1/2}$ for the SEVNB method) were achieved thus breaking through the strength–toughness tradeoff relation in transformation toughened ZrO_2 and its composite materials.[23]

REFERENCES

1. TSUKUMA, K. & SHIMADA, M., Strength, fracture toughness and Vickers hardness of CeO_2-stabilized tetragonal ZrO_2 polycrystals (Ce-TZP). *J. Mater. Sci.*, **20** (1985) 1178–1184.
2. TSUKUMA, K., Mechanical properties and thermal stability of CeO_2 containing tetragonal zirconia polycrystals. *Am. Ceram. Soc. Bull.*, **65** (1986) 1386–1389.
3. TSUKUMA, K., UEDA, K & SHIMADA, M., High-temperature strength and fracture toughness of Y_2O_3-

partially-stabilized ZrO_2/Al_2O_3 composites. *J. Am. Ceram. Soc.*, **68** (1985) C56–C58.
4. TSUKUMA, K., TAKAHATA, T. & SHIOMI, M., Strength and fracture toughness of Y-TZP, Ce-TZP, Y-TZP/Al_2O_3 and Ce-TZP/Al_2O_3. In *Advances in Ceramics, 24, Science and Technology of Zirconia III*. The American Ceramic Society, Westerville, OH, 1988, pp. 721–728.
5. TSAI, J. F., CHON, U., RAMACHANDRAN, N. & SHETTY, D. K., Transformation plasticity, toughening in CeO_2-partially-stabilized zirconia-alumina (Ce-TZP/Al_2O_3) composites doped with MnO. *J. Am. Ceram. Soc.*, **75** (1992) 1229–1238.
6. CULTER, R. A., MAYHEW, R. J., PRETTYMAN, K. M. & VIRKAR, A. V., High-toughness Ce-TZP/Al_2O_3 ceramics with improved hardness and strength. *J. Am. Ceram. Soc.*, **74** (1991) 179–186.
7. MIURA, M., HONGOH, H., YOGO, T., HIRANO, S. & FUJII, T., Formation of plate-like lanthanum–aluminate crystal in Ce-TZP matrix. *J. Mater. Sci.*, **29** (1994) 262–268.
8. NIIHARA, K., NAKAHIRA, A. & HIRAI, T., High temperature properties of Al_2O_3-SiC composites. In *Fracture Mechanics of Ceramics 7*, ed. R. C. Bradt, A. G. Evans, D. P. H. Hasselman & F. F. Lange. Plenum Press, New York, 1985, pp. 103–116.
9. NIIHARA, K., New design concept of structural ceramics — ceramic nanocomposites. *J. Ceram. Soc. Jpn*, **99** (1991) 974–982.
10. NAWA, M., BAMBA, N., SEKINO, T. & NIIHARA, K., The effect of TiO_2 addition on strengthening and toughening in intragranular type of 12Ce-TZP/Al_2O_3 nanocomposites, in press.
11. BROWN, F. H. & DUWEZ, P., The zirconia–Titania system. *J. Am. Ceram. Soc.*, **37** (1954) 129–132.
12. TSUKUMA, K., Transparent TiO_2–Y_2O_3–ZrO_2 ceramics. In *Zirconia Ceramics 8*, ed. S. Somia & M. Yoshimura. Uchida Rokakuho, Japan, 1986, pp. 11–20.
13. GARVIE, R. C. & NICHOLSON, P. S., Phase analysis in zirconia systems. *J. Am. Ceram. Soc.*, **55** (1972) 303–305.
14. NIIHARA, K., MORENA, R. & HASSELMAN, D. P. H., Further reply to "Comment on elastic/plastic indentation damage in ceramics: the median/radial crack system. *J. Am. Ceram. Soc.*, **65** (1982) C–116.
15. AWAJI, H., WATANABE, T. & SAKAIDA, Y., Fracture toughness measurement of ceramics by V notch technique. *Ceram. Int.*, **18** (1992) 11–17.
16. SRAWLEY, J. E., Wide range stress intensity factor expressions for ASTM E 399 standard fracture toughness specimens. *Int. J. Fract.*, **12** (1976) 475–476.
17. GUPTA, T. K., LANGE, F. F. & BECHTOLD, J. H., Effect of stress-induced phase transformation on the properties of polycrystalline zirconia containing metastable tetragonal phase. *J. Mater. Sci.*, **13** (1978) 1464–1470.
18. SWAIN, M. V. & ROSE, L. R. F., Strength limitations of transformation-toughened zirconia alloys. *J. Am. Ceram. Soc.*, **69** (1986) 511–518.
19. HANNINK, R. H. J, MUDDLE, B. C. & SWAIN, M. V., Transformation induced plasticity in tetragonal zirconia polycrystals. *Proc. Austceram 86*. Australian Ceramic Society, Melbourne, 1986, p. 145.
20. ROSE, L. R. F. & SWAIN, M. V., Transformation zone shape in ceria-partially-stabilized zirconia. *Acta Metall.*, **36** (1988) 955–962.
21. YU, C. S., SHETTY, D. K., SHAW, M. C. & MARSHALL, D. B., Transformation zone shape effects on crack shielding in ceria-partially-stabilized zirconia (Ce-TZP)–Alumina composites. *J. Am. Ceram. Soc.*, **75** (1992) 2991–2994.
22. MINATO, I., PEZZOTTI, G. & NIIHARA, K., Microstructure, fracture behavior of Si_3N_4 based ceramic composites. *J. Jpn Soc. Powder & Powder Metall.*, **39** (1992) 1076–1079.
23. SWAIN, M. V. & ROSE, L. R. F., Strength limitations of transformation-toughened zirconia alloys. *J. Am. Ceram. Soc.*, **69** (1986) 511–518.